Doppler Centroid Estimation for ScanSAR Data

Ciro Cafforio, Pietro Guccione, and Andrea Monti Guarnieri

***Abstract*—We introduce a novel accurate technique to estimate the Doppler centroid (DC) in ScanSAR missions. The technique starts from the ambiguous DC measures in the subswaths and uses a method alternative to standard unwrapping to undo the jumps in estimates induced by modulo pulse repetition frequency (PRF) measures. The proposed alternative is less error prone than the usual unwrapping techniques. Doppler Ambiguity is then solved by implementing a maximum-likelihood estimate that exploits the different PRFs used in different subswaths. An azimuth pointing of the antenna that does not change with subswaths, or that changes in a known way, is assumed. However, if the PRF diversity is strong enough, unknown small changes in azimuth pointing are tolerated and accurately estimated. This estimator is much simpler and more efficient, than those in the literature. Results achieved with both RADARSAT 1 and ENVISAT ScanSAR data are reported.**

***Index Terms*—Diversity methods, Doppler measurements, synthetic aperture radar (SAR).**

I. Introduction

An accurate knowledge of the Doppler centroid (DC) is fundamental for synthetic aperture radar (SAR) processing, calibration [1], and even for tracking sensor attitude [2]. In ScanSAR systems, a precise DC estimate is even more important to avoid scalloping, an annoying periodical azimuth modulation of image amplitude. To avoid scalloping, while keeping radiometric error quite less than 0.5 dB, requires accuracy better than 10 Hz [3], [4]. Such accuracy is usually provided in SAR mode, but can hardly be achieved in ScanSAR missions like RADARSAT and ENVISAT wide swath mode (WSM), where the amount of data available in each subswath is up to seven times smaller than in full resolution SAR.

The initial DC guess is obtained, as usual, by the blockwise implementing of a conventional second-order statistic estimate, that derives the antenna pointing from the phase of the first sample of the autocorrelation function (ACF). This space-domain technique, known since the 1950s [5] and refined by Madsen [6], provides a DC estimate with an accuracy quite close to the Cramér bound [7].

However, due to the sampled nature of SAR, such estimates are ambiguous, and retrieve the DC only up to an unknown multiple of the pulse repetition frequency (PRF). The main focus of this paper is to provide an unambiguous range-variant DC measure on which polynomial models, or whatever simple physical model, can be fitted easily.

Manuscript received January 20, 2003; revised June 30, 2003.

C. Cafforio and P. Guccione are with the Dipartimento di Elettrotecnica ed Elettronica, Politecnico di Bari, 4-70125 Bari, Italy.

A. Monti Guarnieri is with the Dipartimento di Elettronica e Informazione, Politecnico di Milano, 32-20133 Milan, Italy (e-mail: monti@elet.polimi.it).

Digital Object Identifier 10.1109/TGRS.2003.817688

The literature reports a wide selection of DC ambiguity-resolving (DAR) techniques, to be used both as blind algorithms, or better combined with estimates made by ephemeris and attitude data, when available. These techniques are based on the following three different principles:

1) DC variation with wavelength, leading to second-order statistical techniques that regress DC measures at different frequencies [8], [9];
2) impact of DC on SAR impulse response (mainly, range migration), leading to high-order spectral (HOS) techniques [10], [11];
3) availability of multiple PRFs, introducing different "wrapped" (or ambiguous) power spectrum measures [3], [12], [13].

The techniques in the third group are the most suited to ScanSAR application. Those in the first group need calibration for a proper "offset frequency" [8], expected to change from beam to beam in ScanSAR mode and even with time, particularly with active antennas, like those of ENVISAT and RADARSAT 2. HOS techniques have poor accuracy and therefore require a large amount of data that should be nongaussian (e.g., with contrast). Such techniques are subject to fail with ScanSAR as the burst mode acquisition limits both the available data and the resolution, hence reducing contrast.

On the other hand, multiple PRF techniques are promising as their accuracy and robustness is increased with the number of different swaths and PRFs. Several implementations have been proposed, either by exploiting the full datasets [12], or by limiting the estimate to the overlap area between subswaths [2], [3], [13]. In this paper, we avoid the latter approach as it would be faulty in missions like ENVISAT-WSM, a five-swath ScanSAR, where the overlap is quite small (less than 5% of the burst range extent), and the DC estimate may be corrupted by the local presence of contrasts or Doppler artifacts (like sea currents). We therefore propose a technique that exploits the whole swath extent and accounts for considerable Doppler drifts in the full imaged range swath. The technique is comparable with the multiple PRF approach in [12] where DC is retrieved by a minimum-mean-square-error (MMSE) technique, nevertheless the technique exploits quite a different estimator.

In the proposed approach, the two consequences of the modulo PRF DC estimation are addressed. The jumps in the DC estimate versus range within a subswath are addressed and resolved first. The problem of DC estimate given a set of ambiguous and noisy measures is converted to the estimation of the phase of a modulated complex sinusoid. The outcome of this first step is a DC estimate that, within each subswath, has no jumps, but is still ambiguous as an unknown number of PRFs are still to be added or subtracted. To solve this second

problem we exploit a maximum-likelihood (ML) technique similar to that used within the context of multibaseline SAR interferometry in [14]. This estimator turns out to be simpler than the exhaustive search (the original Chinese Remainder Theorem), nor does it have the limitations of the suboptimal approach discussed in [12].

The final unambiguous estimates can eventually be used to identify a simple model that expresses their foreseen smooth variations with range and azimuth. The paper assumes simple polynomial models to represent the DC variations with range over all subswaths, depending on the properties of the ScanSAR antenna.

The structure of this paper is straightforward: the technique that combines the interswath unwrapping and the DAR ML estimate is sketched in its essential elements in Section II. The implementation of the DC estimator and the porting to the real cases of RADARSAT 1 and ENVISAT missions, are discussed in Section III, that also presents results achieved by processing real datasets. Conclusions and acknowledgments follow. The Appendix discusses the fitting of a different polynomial in each subswath.

II. Algorithm Rationale

Fig. 1 shows the ScanSAR geometry of ENVISAT WSM, a five-subswath by three looks-per-footprint system. The large swath, usually imaged in ScanSAR mode (100–500 km), accounts for a DC variation due to changes in the relative earth–spacecraft velocity vector.

Spacecraft (S/C) attitude can be used to reduce the Doppler centroid and constrain (almost always) its value within the $[-\text{PRF}/2,\ \text{PRF}/2]$ unambiguous interval. ENVISAT uses this technique, while RADARSAT 1 does not. However, any problem with S/C gyroscopes (e.g., the European Remote Sensing 2 satellite in mono and zero gyro mode since February 2000) invariably translates into DC unpredictability.

Like in any SAR acquisition, the slow time (along-track) sampling at the PRF makes the signal power spectrum periodic. Therefore, DC estimates obtained through techniques that exploit signal power spectrum [5], [6] have an undetermined multiple of PRF added to or subtracted from the true value. To track DC variations with range, the estimation is repeated at all range bins: reaching the boundaries $\pm\text{PRF}/2 + l \cdot \text{PRF}$, for "$l$" integer, jumps of one PRF are experienced. Moreover, in ScanSAR acquisition mode, jumps in the estimated DC will occur at sub swath boundaries because of the different PRF used, unless the true values are all within the smallest $[-\text{PRF}/2,\ \text{PRF}/2]$ interval. The noisiness of the estimates complicates the problem by adding random jumps to the few that would otherwise be experienced, making the "unwrapping" of the estimated DC a nontrvial challenge. The fact is exemplified in Fig. 2.

The algorithm can be thought of as composed of three major steps.

Step 1) PRF jumps within the subswath are removed from the raw estimates through considering the modulo PRF estimate similar to the phase (modulo 2π) of an angle modulated sinusoid.

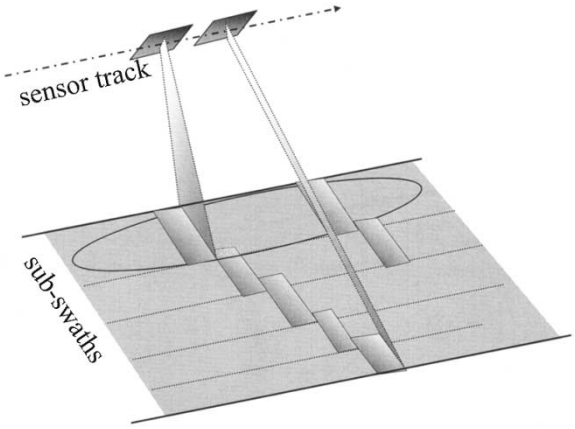

Fig. 1. Typical ScanSAR geometry (here the ENVISAT WSM has been assumed). The antenna is steered electronically to scan subswaths.

Step 2) The absolute DC is estimated by finding, in each subswath, the proper multiple of PRF to be added. An ML technique is introduced to reach this goal.

Step 3) A proper DC versus range model, either polynomial or physical [15], is then fitted to the now-unambiguous measures, giving the final DC estimate.

Let us go into detail by supposing some DC estimates, $\hat{f}_{\text{DCW}}(\tau)$ for each range τ (fast-time), achieved by means of a second-order statistical technique (like [6]). Throughout the paper, the symbol "$\wedge$" is used to denote estimated values. We estimate the first ACF sample, $r(1/\text{PRF}_i)$ (where the index "i" identifies the subswath), by averaging on a block sufficiently small to ignore the azimuth variation of DC (hundreds of lines in a common spaceborne SAR). The simple correlation Doppler centroid estimator (CDCE) is then used

$$\hat{f}_{\text{DCW}_\text{i}} = \arg\left(r\left(\frac{1}{\text{PRF}_i}\right)\right) \cdot \frac{\text{PRF}_i}{(2\pi)} \tag{1}$$

whose accuracy is close to the Cramér–Rao bound [8]. In the following, we will omit the index "i" when we refer to a generic subswath, and we will keep it when reasoning involves more than one subswath.

Let $f_{\text{DC}}(\tau)$ denote the true Doppler centroid frequency versus range time; the ambiguous measures $\hat{f}_{\text{DCW}}(\tau)$ relate to the true DC as follows:

$$\hat{f}_{\text{DCW}}(\tau) + l(\tau) \cdot \text{PRF} = f_{\text{DC}}(\tau) + n(\tau) \tag{2}$$

where $\hat{f}_{\text{DCW}}(\tau)$ is the DC measure at each range bin τ, known in *principal value* (but for multiples of PRF), and l is the unknown integer number of PRFs to add for the true DC. The noise term $n(\tau)$ accounts for all the model and measure errors, whose principal contributions (see [6]–[8] and [16] for a complete analysis) come from the following:

- thermal and quantization noise;
- contrasts in the scene;
- target motion (like on the sea surface);
- saturation and nonlinear distortions.

In most cases, thermal and quantization noises are by far the least influential: their contributions to the variance of the DC estimate can be reduced to a very few Hertz by

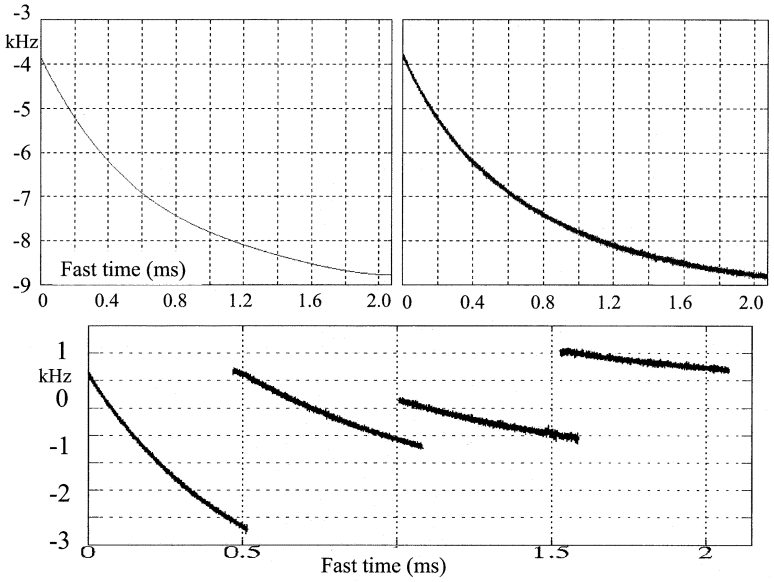

Fig. 2. DC in ScanSAR mode (source: RADARSAT data, wide mode, four beams). The DC, which is range-variant (upper left), is measured in a noisy environment (upper right), and measures are wrapped by the PRF, which changes from swath to swath (bottom). Notice, in this last plot, jumps at swath edges due to PRF switching.

exploiting relatively small blocks [7]. DC accuracy is mostly affected by contrast: any single strong scatterer would provide a directional reflection that jams the estimates of the azimuth antenna pattern as soon as the acquisition is switched on. Compared with conventional SAR, this has a stronger impact, as each scatterer becomes more and more directional as the burst duration shortens. Finally, scenes over the sea experience large, slowly varying, DC shifts of up to several tens of Hertz by ocean currents [17].

A. Estimating DC Within Each Subswath

The first thing to do is to remove the amplitude jumps of $\pm$PRF that may appear in the plot of the estimated (wrapped) DC versus range.

The conventional approach is to take the measures $\hat{f}_{\mathrm{DCW}}(\tau)$ and then unwrap them, removing the jumps. After unwrapping, (2) can be written as

$$\hat{f}_{\mathrm{DCU}}(\tau) + l \cdot \mathrm{PRF} = f_{\mathrm{DC}}(\tau) + n(\tau) \tag{3}$$

where $\hat{f}_{\mathrm{DCU}}(\tau)$ is the unwrapped DC measure, and l is now a constant number within a subswath.

The obvious way to implement this monodimensional unwrapping is to ensure a DC difference between two subsequent range bins smaller than $\mathrm{PRF}/2$ in absolute value. This assumption fails for large sample to sample fluctuations, due to noise $n(t)$, and the failure probability increases as DC gets close to $\mathrm{PRF}/2$. Unwrapping the DC measures is quite dangerous, as a single unwrap error would propagate throughout the whole swath as can be seen in Fig. 3. In other words, an error probability of 1/1000 is enough to risk an incorrect model fit on a swath longer than 1000 range bins.

Note, however, that our problem of dealing with modulo PRF measures is analogous to that of estimating the phase (modulo 2π) of an angle modulated complex sinusoid: $\exp(j2\pi f_{\mathrm{DC}}(\tau)/\mathrm{PRF})$.

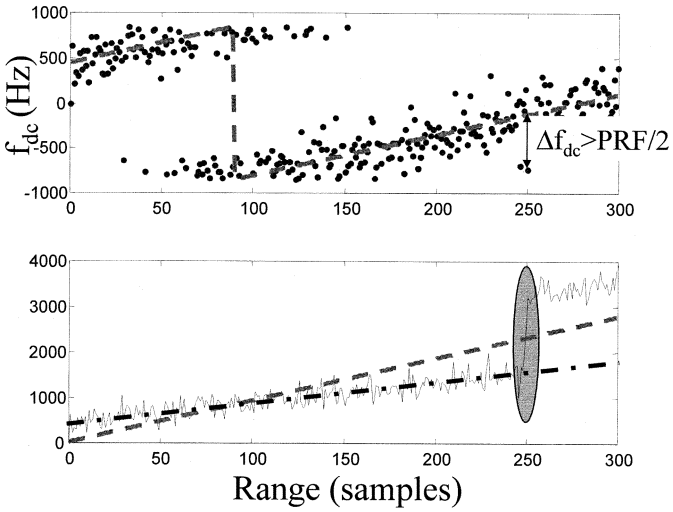

Fig. 3. Effect of unwrapping on the estimate of DC trend (here assumed linear). (Top) Noisy measures and their (wrapped) linear trend. (Bottom) The DC has been unwrapped and then (dashed line) a linear trend fitted. However, the presence of only one unwrap error introduced a large error. The correct DC trend is the one marked with the dashed–dotted line.

Let us assume that the one PRI lag azimuth ACF, r_1, is estimated as a function of range

$$r_1(\tau) = \sum s_r\left(\tau, \frac{t+1}{\mathrm{PRF}}\right) s_r^*(\tau, t) \tag{4}$$

where $s_r(\tau, t)$ is the range-compressed dataset, and the function of fast time τ and slow time t. r_1 is linked to DC by (1)

$$r_1(\tau) = \rho \exp\left(j2\pi \frac{f_{\mathrm{DC}}(\tau)}{\mathrm{PRF}}\right) + w(\tau) \tag{5}$$

ρ being the amplitude that we assume almost constant (we ignore it), and $w(\tau)$ modeling the noise contributions. We assume

$w(\tau)$ to be uncorrelated and Gaussian, due to the summation in (4).

It is quite reasonable to assume that DC variation with range is slow enough to allow a power series expansion in which the constant and linear terms are dominant, at least within the extent of a ScanSAR subswath. Accordingly, we can model the unwrapped DC frequency as

$$f_{\mathrm{DCU}}(\tau) = f_{\mathrm{DC}_0} + \Delta f_{\mathrm{DC}} \cdot \tau + \Delta f(\tau) \tag{6}$$

i.e., by the constant term f_{DC_0}, by the linear term $\Delta f_{\mathrm{DC}} \cdot \tau$ and by the residual higher order terms $\Delta f(\tau)$.

Combining (5) and (6), the variation with range of r_1 can be modeled as

$$\begin{aligned} r_1(\tau) =& \rho \exp\left(j2\pi \frac{f_{\mathrm{DC}_0} + \Delta f_{\mathrm{DC}} \cdot \tau + \Delta f(\tau)}{\mathrm{PRF}}\right) + w(\tau) \\ \simeq& \rho \exp\left(j2\pi \frac{f_{\mathrm{DC}_0} + \Delta f_{\mathrm{DC}} \cdot \tau}{\mathrm{PRF}}\right) + w_t(\tau) \end{aligned}$$

where the higher order terms are included in the "noise" $w_t(\tau)$. We then interpret $r_1(\tau)$ as a complex sinusoid, and the problem is now to estimate its phase and its frequency. In this case, the solution is provided by the minimum variance unbiased estimator [18]

$$\begin{aligned} R_1(f) =& \mathcal{F}(r_1(\tau)) = \int r_1(\tau) \exp(-j2\pi f\tau) d\tau \\ \hat{f}_0 =& \frac{\widehat{\Delta f}_{\mathrm{DC}}}{\mathrm{PRF}} = \arg\left\{ \max_f \left(|R_1(f)|^2 \right) \right\} \\ \hat{\phi}_0 =& \frac{2\pi \hat{f}_{\mathrm{DC}_0}}{\mathrm{PRF}} = \arg\left[R_1\left(\hat{f}_0\right) \right] \end{aligned} \tag{7}$$

$R_1(f)$ being the Fourier transform of $r_1(\tau)$. The estimator (7) can be implemented by means of fast Fourier transform (FFT): an accurate estimate requires data to be zero-padded, so that the FFT is evaluated in a dense grid in the frequency domain. However, as the DC gradient with range is usually small, the chirp-Z transform will do the same job, but much more efficiently [19].

The estimated constant and linear terms can be subtracted directly from the phase of $r_1(\tau)$, leaving what we call "higher order terms" and noise

$$\begin{aligned} \tilde{r}_1(\tau) =& r_1(\tau) \cdot \exp\left\{ -j\left(2\pi \hat{f}_0 \tau + \hat{\phi}_0 \right) \right\} \\ =& \rho \exp\left(j2\pi \frac{\widetilde{\Delta f}(\tau)}{\mathrm{PRF}} \right) \end{aligned}$$

where $\widetilde{\Delta f}(\tau)$ represents the phase of the residual, including both and model errors.

If the residual is such that $|\widetilde{\Delta f}(\tau)| < \mathrm{PRF}/2$ for every τ, its value can be recovered through

$$\widetilde{\Delta f}(\tau) = \frac{\mathrm{PRF}}{2\pi} \arctan\left(\tilde{r}_1(\tau)\right) \tag{8}$$

without any further problem of PRF jumps.

The simple model in (6) that we choose is quite effective, provided that it leaves a residual phase smaller than the unambiguous interval. This condition was verified in all the cases we tested, both with RADARSAT 1 and ENVISAT data. However, if it is believed that the second-order terms could exceed $\mathrm{PRF}/2$, an optimal estimate that still avoids unwrapping can be implemented by means of any SAR autofocusing technique (e.g., see [20]).

In any case, $\widetilde{\Delta f}(\tau)$ will retain residual, smooth variations due to the physical change in sensor-target radial velocity with range, plus noisy fluctuations. Residual smooth variations can be identified through a further model fitting (we used a quadratic polynomial fit), and subtracted, leaving the noise

$$\widetilde{\Delta f}(\tau) = \widehat{\Delta f}(\tau) + n(\tau). \tag{9}$$

B. Solving for DC Ambiguity Intersubswath

Through the use of (6), (7), and (9) the unwrapped estimate for ith subswath $\hat{f}_{\mathrm{DCU}i}(\tau)$ can be expressed as

$$\hat{f}_{\mathrm{DCU}i}(\tau) = \hat{f}_{\mathrm{DC}_0 i} + \widehat{\Delta f}_{\mathrm{DC}i} \cdot \tau + \widehat{\Delta f}_i(\tau) \tag{10}$$

that, with noise [$n(\tau)$ in (9)] added, exactly reproduces the original measures, *without PRF jumps*. However, this unwrapped estimate will differ from the "true" value by an unknown integer multiple of PRF [and by the estimation error $\epsilon_i(\tau)$]. Equation (3) is now written as follows:

$$\hat{f}_{\mathrm{DCU}i}(\tau) + l_i \cdot \mathrm{PRF}_i = f_{\mathrm{DC}}(\tau) + \epsilon_i(\tau). \tag{11}$$

The noise term ϵ_i is the only stochastic component in (11): if (5) holds and model errors are small, its probability distribution is a Rice-phase pdf that we can approximate as a zero-mean normal distribution (for sufficiently high SNR): $N(0, \sigma_n^2)$.

Clearly, there is no way to derive the true DC on the basis of measures in a single swath, as $\hat{f}_{\mathrm{DCU}i}$ is ambiguous and l_i unknown. However, we can solve the problem by exploiting more swaths, sampled with different PRF_i's.

1) ML DC Estimate With Constant Azimuth Pointing: Let us first consider a simple case: the antenna azimuth pointing does not change with subswaths. This means that in the absence of estimation error $\epsilon_i(\tau)$, the unwrapped estimates should match one another exactly at the subswath boundaries, once the correct l_i values are known.

Let us impose the continuity of the DC estimate at the boundary between subswaths i and $i+1$

$$\begin{aligned} f_{\mathrm{DC}}(\tau_{0,i} + \Delta\tau_i) =& \hat{f}_{\mathrm{DCU}i}(\tau_{0,i} + \Delta\tau_i) \\ &+ l_i \cdot \mathrm{PRF}_i - \epsilon_i(\tau_{0,i} + \Delta\tau_i) \\ =& \hat{f}_{\mathrm{DCU}i+1}(\tau_{0,i+1}) \\ &+ l_{i+1} \cdot \mathrm{PRF}_{i+1} - \epsilon_{i+1}(\tau_{0,i+1}) \end{aligned} \tag{12}$$

where swath i is supposed to have width $\Delta\tau_i$ and to start at slant range $\tau_{0,i}$, l_i is the PRF multiplicity in swath i, and the meaning of the other symbols is obvious. Of course, $\tau_{0,i} + \Delta\tau_i = \tau_{0,i+1}$.

This is in contrast with real data, where subswaths overlap: a cross-over point is considered to be any point within the overlapped area. Let us ignore the dependence of noise with time,

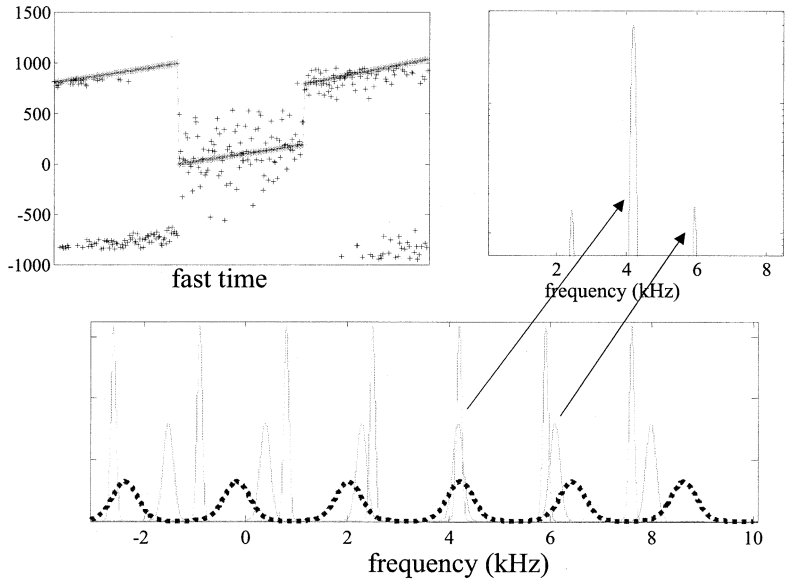

Fig. 4. ML ambiguity estimate. (Upper left) A polynomial model has been fitted in each of the three subswath, thus removing PRF jumps. (Upper right) Superposition of gaussians that approximates the probability (linear scale) of the unambiguous DC in a reference range. (Bottom) The likelihood function (log scale), the product of the Gaussian in the upper right, peaks for the correct DC frequency.

as noise is assumed to be stationary and range bin independent. We can account for a further subswath, $i+2$

$$\begin{aligned} f_{\mathrm{DC}}&(\tau_{0,i}+\Delta\tau_i) \\ &=\hat{f}_{\mathrm{DCUi+2}}(\tau_{0,i+2})+l_{i+2}\cdot\mathrm{PRF}_{i+2}-\epsilon_{i+2}(\tau_{0,i+2})+ \\ &\quad-(f_{\mathrm{DC}}(\tau_{0,i+2})-f_{\mathrm{DC}}(\tau_{0,i+1})) \\ &=\hat{f}_{\mathrm{DCUi+2}}(\tau_{0,i+2})+l_{i+2}\cdot\mathrm{PRF}_{i+2}-\epsilon_{i+2}(\tau_{0,i+2})+ \\ &\quad-\Delta_{i+1}+(\epsilon_{i+1}(\tau_{0,i+1}+\Delta\tau_{i+1})-\epsilon_{i+1}(\tau_{0,i+1})) \quad (13) \end{aligned}$$

where the term Δ_{i+1} is introduced as the difference between the estimated DC at the end and the beginning of each subswath

$$\Delta_{i+1}=\hat{f}_{\mathrm{DCU}i+1}(\tau_{0,i+1}+\Delta\tau_{i+1})-\hat{f}_{\mathrm{DCU}i+1}(\tau_{0,i+1}). \quad (14)$$

Through (13) $f_{\mathrm{DC}}(\tau_{0,1})$ can be related to the vector of the ambiguous measures: $\hat{\mathbf{f}}_{\mathrm{DCU}}=[\hat{f}_{\mathrm{DCU1}}(\tau_{0,1});\hat{f}_{\mathrm{DCU2}}(\tau_{0,2});\ldots]$ and to the unknown integer multipliers: $l=[l_1;l_2;\ldots]$, ending up with the following set of equations:

$$\begin{aligned} f_{\mathrm{DC}}&=f_{\mathrm{DC}}(\tau_{0,1}) \\ &=\hat{f}_{\mathrm{DCU}i}+l_i\cdot\mathrm{PRF}_i-\sum_{k=0}^{i-1}\Delta_k+\bar{\epsilon}_i, \qquad i=1,\ldots,N \end{aligned}$$

with the assumption that $\Delta_0=0$ and that $\bar{\epsilon}_i$ combines all error terms in (13).

Now let us find the ML estimate for the unknown multipliers $\mathbf{l}$. The likelihood function is

$$p_{f_{\mathrm{DC}}|\mathbf{l}}(f_{\mathrm{DC}}\mid\mathbf{l})=\prod_{i=1}^{N}N\left(\hat{f}_{DCi}+l_i\cdot\mathrm{PRF}_i+\Delta_{i+1},\sigma^2_{\epsilon_i}\right). \quad (15)$$

N is the normal distribution already introduced in Section II-B. The set $\{l_i\}$ that maximizes (15) gives the solution to the ambiguity problem. The solution searched can be limited to all the integer values in a reasonable interval: $l_{\mathrm{MIN}}<l_i<l_{\mathrm{MAX}}$. This would be as a very rough model for $p(\mathbf{l})$ a better prior probability could be derived by a careful modeling of the sensor attitude with orbits.

TABLE I
PARAMETERS OF RADARSAT IN SCANSAR NARROW MODE

Acquisition date		July 16, 2001
range sampling frequency f_s [MHz]		12.92683
number of bursts used for estimation		10
number of echo pulses per burst		112
overlapped region [samples]		450
	SS1	SS2
PRF [Hz]	1295.53	1332.39
range samples	6672	7944

Even though the problem is solved, it is useful to delve a little deeper, to gain more insight. Knowledge of $p(\mathbf{l})$ can transform the conditional probability density function (pdf) (15) into the joint pdf and, summing over all $\mathbf{l}$, the marginal pdf for f_{DC} is obtained. By inspection

$$\begin{aligned} p_{f_{\mathrm{DC}}}(f_{\mathrm{DC}})&=\prod_{i=1}^{N}p_{f_{\mathrm{DC}}i}(f_{\mathrm{DC}}) \\ &=\prod_{i=1}^{N}\sum_{l_i=l_{\mathrm{MIN}}}^{l_{\mathrm{MAX}}}N\left(\hat{f}_{\mathrm{DCi}}+l_i\mathrm{PRF}_i+\Delta_{i+1},\sigma^2_{\epsilon_i}\right) \end{aligned} \quad (16)$$

i.e., the pdf for $p_{f_{\mathrm{DC}}}(f_{\mathrm{DC}})$ is the product of the marginal pdf of f_{DC} estimated through measures within one subswath. Obviously, these are periodic as values differing by multiples of PRF_i are equally likely. The final result (16) will be periodic, too. However, this period must be common to all $p_{f_{\mathrm{DC}}i}$'s, and it is the minimum common multiple between the PRFs in all subswaths (they are usually integer fractions of a common clock frequency).

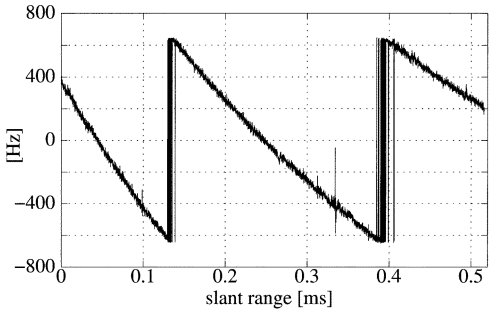

Fig. 5. Raw Doppler centroid estimate (first subswath).

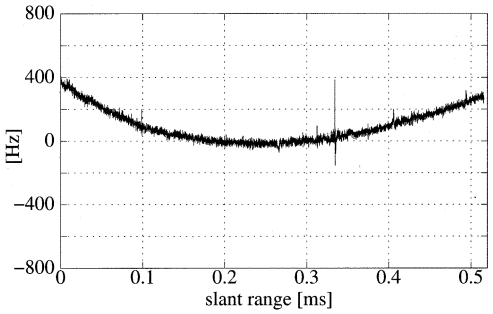

Fig. 6. Residual Fig. 5 after linear trend removal.

The maximum of (16) marks the most probable value for f_{DC}. From this, l_i can be retrieved. An example of such a technique is given in Fig. 4.

Confidence in the result can be assessed simply. In fact, the marginal density function will have a very high peak where f_{DC} is located, but also secondary maxima may exist. Their relative amplitudes can be used to verify that the set of PRFs is adequate to solve the ambiguity problem. It is worth noting that such information provides clues to both the probability error (the intensity of the peak) and error itself (the position of the peak).

2) ML DC Estimate With Varying Azimuth Pointing: Modern phased antenna arrays are subject to variation of azimuth pointing throughout all the subswath. For example, Doppler centroid jumps from swath to swath are evident in ENVISAT data: such jumps are due to the active antenna behavior and cannot be ascribed to ambiguous measurements.

This being the case, the treatment of Section II-B1 must be modified, and two different situations can be envisaged.

- Jumps in azimuth pointing are systematic and, therefore, accurately modeled.
- Nothing is known about the pointing changes, or these changes vary with time due to system aging, system failure, etc.

The first situation is dealt with in an obvious way: pointing jumps can be transformed into Doppler shifts with sufficient accuracy. Let these DC jumps be $\delta_{i,i+1}(f_{\mathrm{DC}})$ and considered as additional contributions in (12), that now become

$$\hat{f}_{\mathrm{DCU}i}\left(\tau_{0,i}+\Delta\tau_i\right)+l_i\cdot\mathrm{PRF}_i-\epsilon_i\left(\tau_{0,i}+\Delta\tau_i\right)$$
$$=\hat{f}_{\mathrm{DCU}i+1}\left(\tau_{0,i+1}\right)+l_{i+1}\cdot\mathrm{PRF}_{i+1}-\epsilon_{i+1}\left(\tau_{0,i+1}\right)+\delta_{i,i+1}\left(f_{\mathrm{DC}}\right).$$

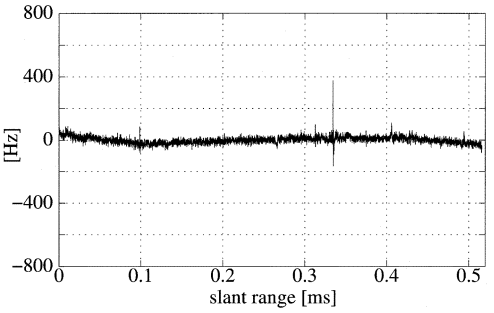

Fig. 7. Residual in Fig. 6 after second-order polynomial fit removal.

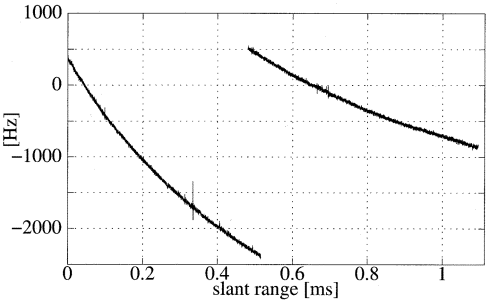

Fig. 8. Plots of the unwrapped Doppler estimates for narrow mode: both subswaths.

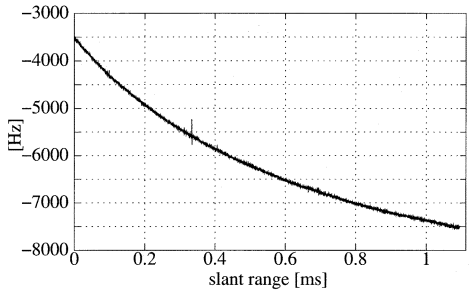

Fig. 9. Final result for narrow mode.

If the pointing changes are unknown and the induced Doppler shifts are small with respect to the PRF differences between consecutive subswaths, the algorithm will still be able to resolve the ambiguity: however, in evaluating the estimation variances $\sigma^2_{\epsilon_i}$ jumps must be considered.

C. Model Fitting

The ML provides an evaluation of both the reference DC, and the number of ambiguities to be added in each subswath, l_i. Once the ambiguity is resolved, we have the original measures, unwrapped and with ambiguity removed, but with the full complement of measurement noise.

Having removed the problem of the DC wrapping, we are now able to fit the *unwrapped* measures to a suitable model to provide the final DC estimate. However, the choice of the model is beyond the scope of this paper. We could, for example, use a physical approach, that links the DC to the attitude of the sensor [17], or performs a tracking of the attitude if large strips of data are available [2] or, simply, assume a polynomial model (the simplest and usual choice, for which a few experimental results are shown).

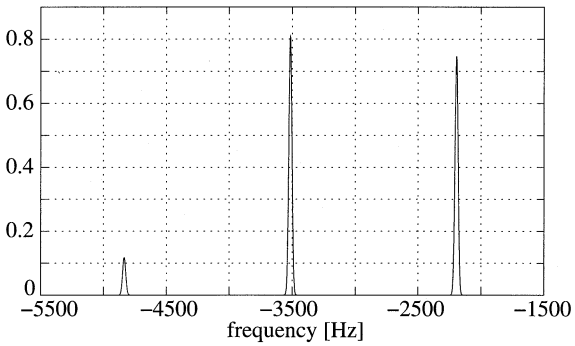

Fig. 10. Joint pdf for the ScanSAR narrow mode.

D. Limitations

The proposed algorithm is more robust than algorithms that exploit overlap areas, as it exploits the whole swath. Moreover, it is much simpler than techniques that exploit the Chinese Remainder theorem trying to minimize directly the MMSE. Finally, with this algorithm it is possible to tune the variances σ_i^2 in (15) in order to adapt to DC estimates with different accuracies.

Two conditions must be met to guarantee good performances. The first one is that the statistical fluctuations in the initial clutterlock estimates and the quadratic and higher order terms in DC variation with range are small enough to prevent residual PRF jumps after the spectral estimation/compensation step is carried out. This condition is expected to hold, if enough reasonable quality data are available, also for acquisitions for which large DC variation with range are experienced. The second condition is that the differences in PRF are larger than the errors in the intra subswath DC models.

III. Experimental Results

The algorithm has been successfully tested on real data from two RADARSAT 1 and several ENVISAT wide swath mode missions.

A. Radarsat 1

The data refer to two RADARSAT 1 acquisitions over Quebec, Canada, in the summer of 2001, in the two available ScanSAR modes: narrow (two subswaths) and wide (four subswaths). Without yaw steering, the DC for RADARSAT varies considerably around the orbit and may have very large values. The large f_{DC} variation and the presence of a quadratic term are clearly visible for both acquisition modes.

1) Narrow Mode: Relevant mission parameters are summarized in Table I.

A strip of $\simeq 1000$ range focused lines with land returns was fed into the algorithm to obtain the "wrapped" DC estimates for each sub swath (Fig. 5 shows the result for the first swath in Narrow mode). The residuals after the linear and second-order term removal, plotted in Figs. 6 and 7, are quite small and well below the PRF/2 limit. This allowed for the proper unwrapping of the *DC* within each of the two subswaths, shown in Fig. 8. The final result, after PRF ambiguity removal, is shown in Fig. 9.

The narrow mode acquisition just discussed represents an extreme case for PRF diversity: the two PRFs used differ only by ~ 36 Hz. It is even surprising that the ML algorithm gives a reasonable solution. The joint probability density function shown in Fig. 10 has only one secondary maximum of level comparable to that of the global maximum. Due to the small difference in the PRF, any data "irregularity" (at the start of the scene there is a sea inlet with little or no backscattering) could switch the two maxima.

This, in turn, would impair the algorithm potential for automation. To reach the solution that guarantees a seamless joining of the DC estimates, one further step is added to the processing, that compares the sets of ambiguities identified by the absolute maximum, and by secondary maxima, whenever these are higher than, say, 50% of the global value. The set that exhibits the minimum-mean-square error (MMSE). between neighboring estimates in overlapping regions is considered the correct choice. This strategy works for RADARSAT 1 as a constant azimuth pointing is expected.

To check that the "seamless joining" strategy was correct, the results after two azimuth focusing, performed by assuming the two Doppler centroid values (that differ for one ambiguity) have been compared. Fig. 11 shows details of a point scatterer focused with the DC in the correct replica and with a wrong DC replica, corresponding to the second peak in Fig. 10. This

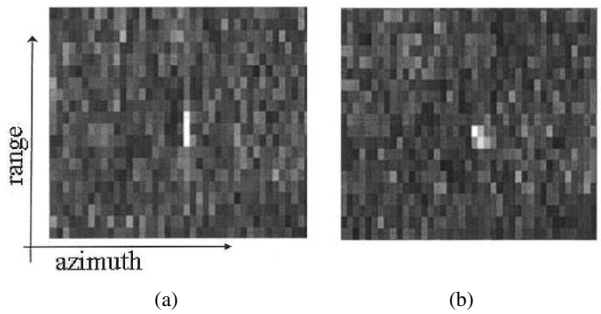

Fig. 11. Details of a point scatterer focused with (a) the DC in the correct replica and (b) with a wrong DC replica.

TABLE II
PARAMETERS OF RADARSAT IN SCANSAR WIDE MODE

Acquisition date				August 11, 2001
range sampling frequency f_s [MHz]				12.92683
number of bursts used for estimation				18
number of echo pulses per burst				58
	SS1	SS2	SS3	SS4
PRF [Hz]	1295.53	1334.86	1233.24	1277.10
range samples	6672	7944	7536	7072
overlap	612	1002	792	

TABLE III
PARAMETERS OF ENVISAT IN WIDE SWATH MODE

Acquisition date				October 2, 2002	
range sampling frequency f_s [MHz]				19.207680	
number of bursts used for estimation				20	
	SS1	SS2	SS3	SS4	SS5
PRF [Hz]	1684.88	2102.41	1692.60	2080.55	1707.04
echoes/burst	50	80	67	87	74
range samples	6344	5089	6234	5104	6018
overlap	340	385	670	480	

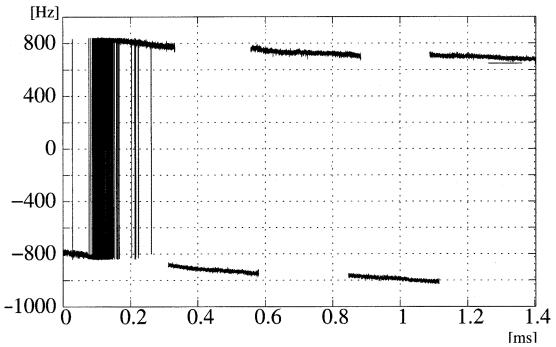

Fig. 12. ENVISAT wide swath mode. Plots of the raw Doppler estimates.

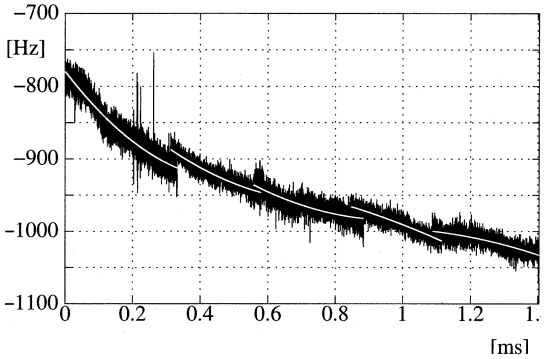

Fig. 13. Final result for wide swath mode. An independent second-order polynomial has been fitted in each subswath.

second image shows the marked diagonal artifact typical of DC ambiguity error [11].

2) Wide Mode: Relevant mission parameters are summarized in Table II.

The intrasubswath unwrapped estimates and the final result are those already shown in Fig. 2. Here, the presence of four PRF, though differing slightly one from the other, made the ambiguity resolution less problematic. In fact no search between neighboring solutions was necessary.

B. ENVISAT Wide Swath Mode

Relevant mission parameters are summarized in Table III.

Usually, yaw steering keeps Doppler shift within the nonambiguous interval. This dataset was selected just because the $-\mathrm{PRF}/2$ limit was exceeded, as shown in Fig. 12. The residual curvature of DC estimate versus range within one subswath is so small that there was no visible difference between the figures analogous to Figs. 6 and 7.

PRFs in odd numbered subswaths differ from those in even numbered ones by $\simeq 500$ Hz, and this makes the job of the ambiguity resolver much easier. This is fortunate as, due to the active phased array antenna of ENVISAT, there is no way to obtain continuity in Doppler estimates for contiguous subswaths. DC jumps are due to small azimuth pointing changes. However, due to the large PRF changes, the ML algorithm is still able to obtain the correct solution (as the seamless mosaicking of neighboring subswaths in processed images demonstrates).

However, changing azimuth pointing with subswaths complicates the compaction of the DC measures into a simple model

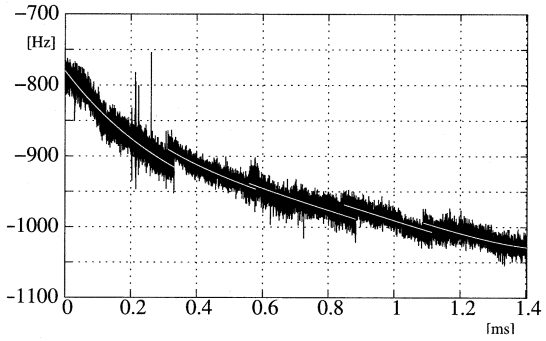

Fig. 14. Final result for wide swath mode. A fourth-order polynomial has been fitted after resolving for DC ambiguity.

(be it polynomial or not). It is obvious that only one polynomial fitting over the whole swath cannot be used. A different polynomial fit over each subswath (see Fig. 13) gives solutions that are too dependant on the local backscattering structure. A more regular result is obtained if the different polynomials are allowed to change only in their constant terms, as Fig. 14 shows.

IV. Conclusion

A practical and very simple method to estimate the nonambiguous Doppler centroid versus slant range for ScanSAR sensors has been presented. The method combines an efficient intrasubswath unwrapping, based on spectral analysis, with a DC ambiguity resolver, based on the maximum-likelihood criterion, that exploits the different PRFs used in subswaths. Tests were conducted with success on a limited set of RADARSAT (narrow and wide mode) and ENVISAT (WSM) datasets, although in some of them limit conditions we be reached.

Appendix
Multiple Polynomials Fitting

If DC variation with range can be expressed as

$$f_{\mathrm{cd}}(x) = \sum_{k=0}^{N} p(k) \cdot x^k$$

to find the MMSE fit to the measured values $\hat{f}_{\mathrm{cd}}$, the set of p's that satisfies

$$\sum_{x \in \text{all ss}} \left(\sum_{k=0}^{N} p(k) \cdot x^k - \hat{f}_{\mathrm{cd}}(x) \right)^2 = \min \qquad (17)$$

must be searched.

The DC measures obtained with the ENVISAT data seem to require a different fit in each subswath. Equation (17) could be applied to each subswath independently of the others, giving a different set of coefficients for each subswath. Experimental results show that this procedure gives bad results even with well behaved data.

The underlying physical model requires a smooth change of Doppler centroid with range. The different azimuth antenna pointing in each subswath can justify the jumps in the value of f_{cd}. The idea is that all the polynomial coefficients must

be the same throughout the whole swath, but for the constant term. At the subswath boundaries only a step change can be allowed. How to find the best polynomial approximation and the stepwise changes? A different polynomial is assumed for each subswath, with coefficients $p_1(0)\cdots p_1(N)$ for the first, $p_2(0)\cdots p_2(N)$ for the second and so on. However, these coefficient sets differ only in their first components, i.e., the constant terms. The unknowns are

$$\mathbf{p} = [p_1(0)\, p_2(0)\cdots p_M(0)\, p(1)\, p(2)\cdots p(N)]$$

supposing that the polynomial degree is N and that the number of swaths is M, and they must satisfy the following condition:

$$\sum_{x\in \mathrm{ss}1}\left(\sum_{k=0}^{N} p_1(k)\cdot x^k - \hat{f}_{\mathrm{cd}}(x)\right)^2 + \sum_{x\in \mathrm{ss}2}\left(\sum_{k=0}^{N} p_2(k)\cdot x^k - \hat{f}_{\mathrm{cd}}(x)\right)^2 + \cdots + \sum_{x\in \mathrm{ss}M}\left(\sum_{k=0}^{N} p_M(k)\cdot x^k - \hat{f}_{\mathrm{cd}}(x)\right)^2 = \min. \tag{18}$$

Remembering that $p_l(k) = p(k)$ for $k \geq 1$ and that (18) implies that all derivatives with respect to all p's must be zero

$$\begin{aligned}
&\sum_{x\in \mathrm{ss}1}\left(\sum_{k=0}^{N} p_1(k)\cdot x^k - \hat{f}_{\mathrm{cd}}(x)\right) = 0\\
&\qquad\vdots\\
&\sum_{x\in \mathrm{ss}M}\left(\sum_{k=0}^{N} p_M(k)\cdot x^k - \hat{f}_{\mathrm{cd}}(x)\right) = 0\\
&\sum_{j=1}^{M}\left(\sum_{x\in \mathrm{ss}j}\left(\sum_{k=0}^{N} p_j(k)\cdot x^k - \hat{f}_{\mathrm{cd}}(x)\right)\cdot x\right) = 0\\
&\qquad\vdots\\
&\sum_{j=1}^{M}\left\{\sum_{x\in \mathrm{ss}j}\left(\sum_{k=0}^{N} p_j(k)\cdot x^k - \hat{f}_{\mathrm{cd}}(x)\right)\cdot x^N\right\} = 0.
\end{aligned}$$

In matricial form

$$\begin{bmatrix}\mathbf{A} & \mathbf{B}^T\\ \mathbf{B} & \mathbf{C}\end{bmatrix}\mathbf{p} = \mathbf{d} \tag{19}$$

where ^{T} denotes transpose where $\mathbf{A}[M\times M]$ is a diagonal matrix whose elements are

$$\mathbf{A} = \mathrm{diag}\left(\sum_{x\in \mathrm{ss}1} 1; \sum_{x\in \mathrm{ss}2} 1; \cdots; \sum_{x\in \mathrm{ss}M} 1\right)$$

and $\mathbf{B}[N\times M]$, $\mathbf{C}[N\times N]$ and $\mathbf{d}[1\times(M+N)]$ are so defined

$$\mathbf{B} = \begin{bmatrix} \sum_{x\in \mathrm{ss}M} x & \vdots & \sum_{x\in \mathrm{ss}M} x\\ \cdots & \vdots & \cdots\\ \sum_{x\in \mathrm{ss}1} x^N & \vdots & \sum_{x\in \mathrm{ss}M} x^N\end{bmatrix}$$

$$\mathbf{C} = \begin{bmatrix} \sum_{x\in \mathrm{ss}M} x^2 & \vdots & \sum_{x\in \mathrm{all\ ss}} x^{N+1}\\ \cdots & \vdots & \cdots\\ \sum_{x\in \mathrm{all\ ss}} x^{N+1} & \vdots & \sum_{x\in \mathrm{all\ ss}} x^{2N}\end{bmatrix}$$

$$\mathbf{d}^T = \begin{bmatrix} \sum_{x\in \mathrm{all\ ss}} \hat{f}_{dc}(x) & \cdots & \sum_{x\in \mathrm{ss}M} \hat{f}_{dc}(x)\\ \sum_{x\in \mathrm{ss}M} x\cdot \hat{f}_{dc}(x) & \cdots & \sum_{x\in \mathrm{all\ ss}} x^N\cdot \hat{f}_{dc}(x)\end{bmatrix}.$$

The solution of (19) produces the experimental results shown in Fig. 14.

The procedure can be generalized to allow also linear terms to change for polynomials in different subswaths.

ACKNOWLEDGMENT

The authors wish to thank ESA and Telespazio S.p.A. for providing the data.

REFERENCES

[1] J. C. Curlander and R. N. McDonough, *Synthetic Aperture Radar: Systems and Signal Processing*. New York: Wiley, 1991.
[2] M. V. Dragosevic and B. Plache, "Doppler tracker for a spaceborne ScanSAR system," *IEEE Trans. Aerosp. Electron. Syst.*, vol. 36, pp. 907–924, July 2000.
[3] M. Y. Jin, "Optimal range and Doppler centroid estimation for a ScanSAR system," *IEEE Trans. Geosci. Remote Sensing*, vol. 34, pp. 479–488, Mar. 1996.
[4] R. Bamler, "Optimum look weighting for burst-mode and ScanSAR processing," *IEEE Trans. Geosci. Remote Sensing*, vol. 33, pp. 722–725, May 1995.
[5] T. B. Pickard, "The effect of noise upon a method of frequency measurement," *IRE Trans. Inform. Theory*, vol. IT, pp. 83–88, June 1958.
[6] S. N. Madsen, "Estimating the Doppler centroid of SAR data," *IEEE Trans. Aerosp. Electron. Syst.*, vol. 25, pp. 134–140, Mar. 1989.
[7] R. Bamler, "Doppler frequency estimation and the Cramèr–Rao bound," *IEEE Trans. Geosci. Remote Sensing*, vol. 29, pp. 385–390, May 1991.
[8] R. Bamler and H. Runge, "PRF-ambiguity resolving by wavelength diversity," *IEEE Trans. Geosci. Remote Sensing*, vol. 29, pp. 997–1003, Nov. 1991.
[9] F. Wong and I. G. Cumming, "A combined SAR Doppler centroid estimation scheme based upon signal phase," *IEEE Trans. Geosci. Remote Sensing*, vol. 34, pp. 696–707, May 1996.
[10] I. G. Cumming, P. F. Kavangh, and M. R. Ito, "Resolving the Doppler ambiguity for spaceborne synthetic aperture radar," in *Proc. IGARSS*, Zurich, Switzerland, 1986, pp. 1649–1653.
[11] C. Prati, F. Rocca, Y. Kost, and E. Damonti, "Blind deconvolution for Doppler centroid estimation," *IEEE Trans. Geosci. Remote Sensing*, vol. 29, pp. 934–941, Nov. 1991.
[12] C. Y. Chang and J. C. Curlander, "Application of the multiple PRF technique to resolve Doppler centroid estimation ambiguity for spaceborne SAR," *IEEE Trans. Geosci. Remote Sensing*, vol. 30, pp. 941–949, Sept. 1992.
[13] C. S. Purry, K. Dumper, G. C. Verwey, and S. R. Pennock, "Resolving Doppler ambiguity for scanSAR data," in *Proc. IGARSS*, Honolulu, HI, July 24–28, 2000, pp. 2272–2274.
[14] A. Ferretti, A. Monti Guarnieri, C. Prati, and F. Rocca, "Multi baseline interferometric techniques and applications," in *Proc. FRINGE 96' Workshop on ERS SAR Interferometry*, Zürich, Switzerland, Sept. 30–Oct. 2 1996.
[15] S. R. Marandi, "Radarsat attitude estimates based on Doppler centroid measurements," in *Proc. CEOS SAR Workshop*, St. Hubert, QC, Canada, Feb. 4–6, 1997, p. 13.

[16] M. Y. Jin, "Optimal Doppler centroid estimation for a SAR data from a quasihomogenous source," *IEEE Trans. Geosci. Remote Sensing*, vol. 24, pp. 1022–1025, Mar. 1986.
[17] W. Hughes and M. W. A. van der Kooij, "Current estimation using burst mode data," in *Proc. 4th Eur. Conf. Synthetic Aperture Radar*, Cologne, Germany, June 4–6, 2002, pp. 121–124.
[18] S. M. Kay, *Fundamentals of Statistical Signal Processing*. Upper Saddle River, NJ: Prentice-Hall, 1993, vol. 1, Estimation Theory.
[19] A. V. Oppenheim and R. W. Schafer, *Discete-Time Signal Processing*. Upper Saddle River, NJ: Prentice-Hall, 1989.
[20] E. Wahl, P. H. Eichel, D. C. Ghiglia, and C. V. Jakowatz, "Phase gradient autofocus: A robust tool for high resolution SAR phase correction," *IEEE Trans. Aerosp. Electron. Syst.*, vol. 30, pp. 827–835, July 1994.

Ciro Cafforio received the laurea degree from the Politecnico di Milano, Milan, Italy, in 1973.

He was a Researcer and Teacher with the Politecnico di Milano until 1987, when he moved to the Politecnico di Bari, Bari, Italy. He is currently Full Professor. He is interested in digital signal processing. He has worked mainly on motion-compensated television coding and on synthetic aperture radar signal processing.

Pietro Guccione was born in 1971 in Bari, Italy. He received the laurea degree in electronic engeineering and the Ph.D. degree from the Politecnico di Bari, in 1996 and 2001, respecitvely.

He is currently an Assistant in the Dipartimento di Elettrotecnica ed Elettronica, Politecnico di Bari. His main interests and publications are in SAR and ScanSAR focusing and interferometry.

Andrea Monti Guarnieri was born in Milan, Italy, on February 9, 1962. He received the laurea degree in electronic engineering from the Politecnico di Milano, in 1988.

Since 1988, he has been with the Dipartimento di Elettrotecnica ed Elettronica, Politecnico di Milano, where he joined the Digital Signal Processing team, and he is currently an Associate Professor. He teaches courses on signal theory, signals and systems, and radar theory and techniques. His research interests concern digital signal processing, mainly in the field of synthetic aperture radar signal processing. Since 1987, he has authored more than 50 scientific publications in the field of synthetic aperture radar.

Prof. Monti Guarnieri was awarded the Symposium Paper Award at the IGARSS in 1989.